

# The Lyman- $\alpha$ forest in $f(R)$ modified gravity

Christian Arnold<sup>1,2</sup>, Ewald Puchwein<sup>3,1</sup> and Volker Springel<sup>1,4</sup>

<sup>1</sup>Heidelberger Institut für Theoretische Studien, Schloss-Wolfsbrunnengasse 35, 69118 Heidelberg, Germany

<sup>2</sup>Institut für Theoretische Physik, Philosophenweg 16, 69120 Heidelberg, Germany

<sup>3</sup>Institute of Astronomy and Kavli Institute for Cosmology, University of Cambridge, Madingley Road, Cambridge CB3 0HA, UK

<sup>4</sup>Zentrum für Astronomie der Universität Heidelberg, Astronomisches Recheninstitut, Mönchhofstr. 12-14, 69120 Heidelberg, Germany

November 12, 2014

## ABSTRACT

In this work, we analyze the Lyman- $\alpha$  forest in cosmological hydrodynamical simulations of chameleon-type  $f(R)$  gravity with the goal to assess whether the impact of such models is detectable in absorption line statistics. We carry out a set of hydrodynamical simulations with the cosmological simulation code MG-GADGET, including star formation and cooling effects, and create synthetic Lyman- $\alpha$  absorption spectra from the simulation outputs. We statistically compare simulations with  $f(R)$  and ordinary general relativity, focusing on flux probability distribution functions (PDFs) and flux power-spectra, an analysis of the column density and line width distributions, as well as the matter power spectrum. We find that the influence of  $f(R)$  gravity on the Lyman- $\alpha$  forest is rather small. Even models with strong modifications of gravity, like  $|\bar{f}_{R0}| = 10^{-4}$ , do not change the statistical Lyman- $\alpha$  properties by more than 10%. The column density and line width distributions are hardly affected at all. It is therefore not possible to get competitive constraints on the background field  $f_R$  using current observational data. An improved understanding of systematics in the observations and a more accurate modeling of the baryonic/radiative physics would be required to allow this in the future. The impact of  $f(R)$  on the matter power spectrum in our results is consistent with previous works.

**Key words:** cosmology: theory – methods: numerical

## 1 INTRODUCTION

Theoretically explaining the late time accelerated expansion of the Universe is one of the biggest challenges in modern cosmology. In the standard model of cosmology, the  $\Lambda$  cold dark matter ( $\Lambda$ CDM) model, the cosmological constant  $\Lambda$  is responsible for the acceleration. While the  $\Lambda$ CDM model is quite successful in explaining many aspects of cosmic structure formation, it also features some problems, one of them being the lack of a natural explanation for  $\Lambda$ . This encourages the search for alternative theories.

In general, the models attempting to provide a theoretical explanation for the accelerated expansion can be divided into two main classes. The first class, which also includes  $\Lambda$ CDM, contains so-called *dark energy* models. These models add a new type of “matter” to the energy-momentum tensor of general relativity (GR). If this type of matter is described by an equation of state with a negative effective pressure, it can drive the accelerated expansion.

The second class are the so-called *modified gravity* models. To explain the accelerated expansion, they modify the gravitational interaction. In other words: while the dark en-

ergy models change the right hand side of Einstein’s equation, the modified gravity models modify its left hand side.

In this work we consider  $f(R)$ -gravity, which can be viewed as a member of the second class. The modification to gravity is carried out by adding a scalar function of the Ricci scalar  $R$  to the action of GR. Because GR is well tested in our local environment, particularly in the solar system, modified gravity theories typically share the need for some screening mechanism which suppresses the modification of GR in high density environments. Examples for such screening mechanisms are the *Chameleon* (Khoury & Weltman 2004), the *Symmetron* (Hinterbichler & Khoury 2010), the *Vainshtein* (Vainshtein 1972) or the *Dilaton* (Gasperini et al. 2002) mechanism. In  $f(R)$  gravity, the screening mechanism is determined by the particular choice of  $f(R)$ . We here consider a model proposed by Hu & Sawicki (2007), which gives rise to a Chameleon mechanism.

Previous simulation works on chameleon-type  $f(R)$ -gravity mainly employed collisionless simulations, analyzing, e.g., halo mass functions (e.g. Schmidt et al. 2009; Ferraro et al. 2011; Zhao et al. 2011; Li & Hu 2011), matter power spectra (e.g. Oyaizu 2008; Li et al. 2012, 2013; Puchwein et al. 2013; Llinares et al. 2014), density profiles (Lombriser

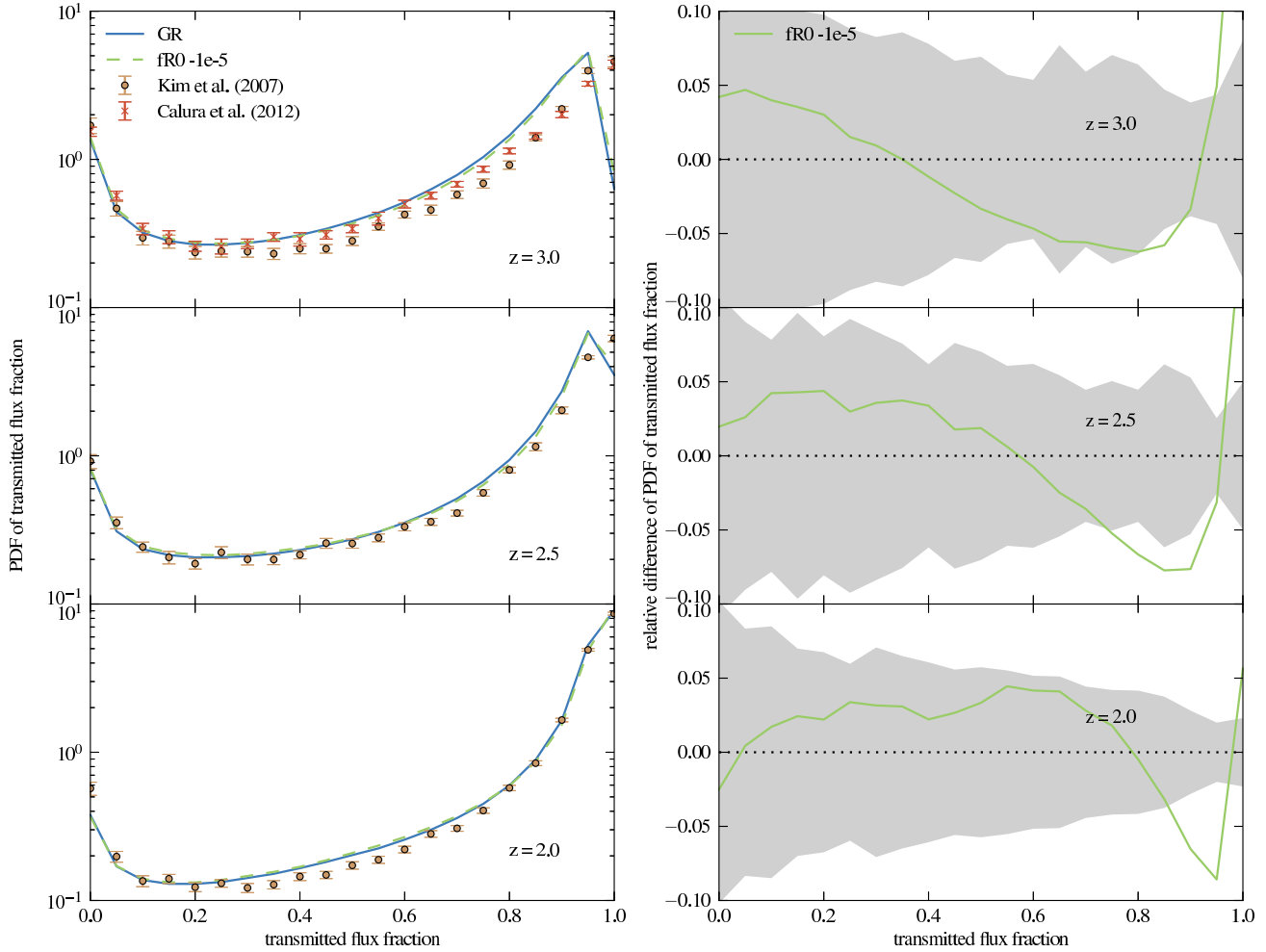


**Figure 1.** *Left panel:* PDF of the transmitted flux fraction for different redshifts for  $\Lambda$ CDM and  $|\bar{f}_{R0}| = 10^{-5}$ , using the results of the large simulation boxes. The dots with errorbars show the data of Kim et al. (2007). For  $z = 3$ , the observational results of Calura et al. (2012) are shown in addition (we plot the “no metals, no LLS” values of this work here). *Right panel:* relative difference of the PDFs on the left hand side. The shaded regions show the  $1\sigma$  relative errors of the observational results of Kim et al. (2007). The mean transmission is tuned to the values of this work in both panels.

et al. 2012b; Corbett Moran et al. 2014), cluster concentrations (Lombriser et al. 2012a), the integrated Sachs-Wolfe effect (Cai et al. 2014), redshift space distortions (Jennings et al. 2012), velocity dispersions (Schmidt 2010; Lombriser et al. 2012a; Lam et al. 2012; Arnold et al. 2014), the impact of screening on the fifth force in galaxy clusters (Corbett Moran et al. 2014) and galaxy populations which were followed with a semi-analytical model (Fontanot et al. 2013). Using hydrodynamical simulations instead, we studied in previous work (Arnold et al. 2014) the temperature of the intracluster medium and different mass measures of galaxy clusters.

In this work, we will for the first time extend the analysis of hydrodynamical  $f(R)$  modified gravity simulations to the statistical properties of the Lyman- $\alpha$  forest. Employing the modified gravity simulation code MG-GADGET we carry out simulations to redshift  $z = 2$ , given that most Lyman- $\alpha$  data lies at redshifts  $z \sim 2 - 4$ . Creating synthetic Lyman- $\alpha$  absorption spectra from the simulation outputs,

we present an analysis of flux PDFs, flux power spectra, line shape statistics, as well as of the matter power spectrum for both  $f(R)$ -gravity and an ordinary  $\Lambda$ CDM model. We particularly focus on the relative differences between these two cosmogonies and compare our results to observations.

This paper is structured as follows. In Section 2, we give a brief summary of the particular parameterization of  $f(R)$  we adopt, whereas Section 3 describes the simulation set we have carried out. In Section 4, we present our main results. Finally, we give a summary and our conclusions in Section 5.

## 2 $f(R)$ -GRAVITY

$f(R)$  gravity models can explain the late time accelerated expansion of the Universe without a cosmological constant. Using the framework of Einstein’s general relativity (GR),

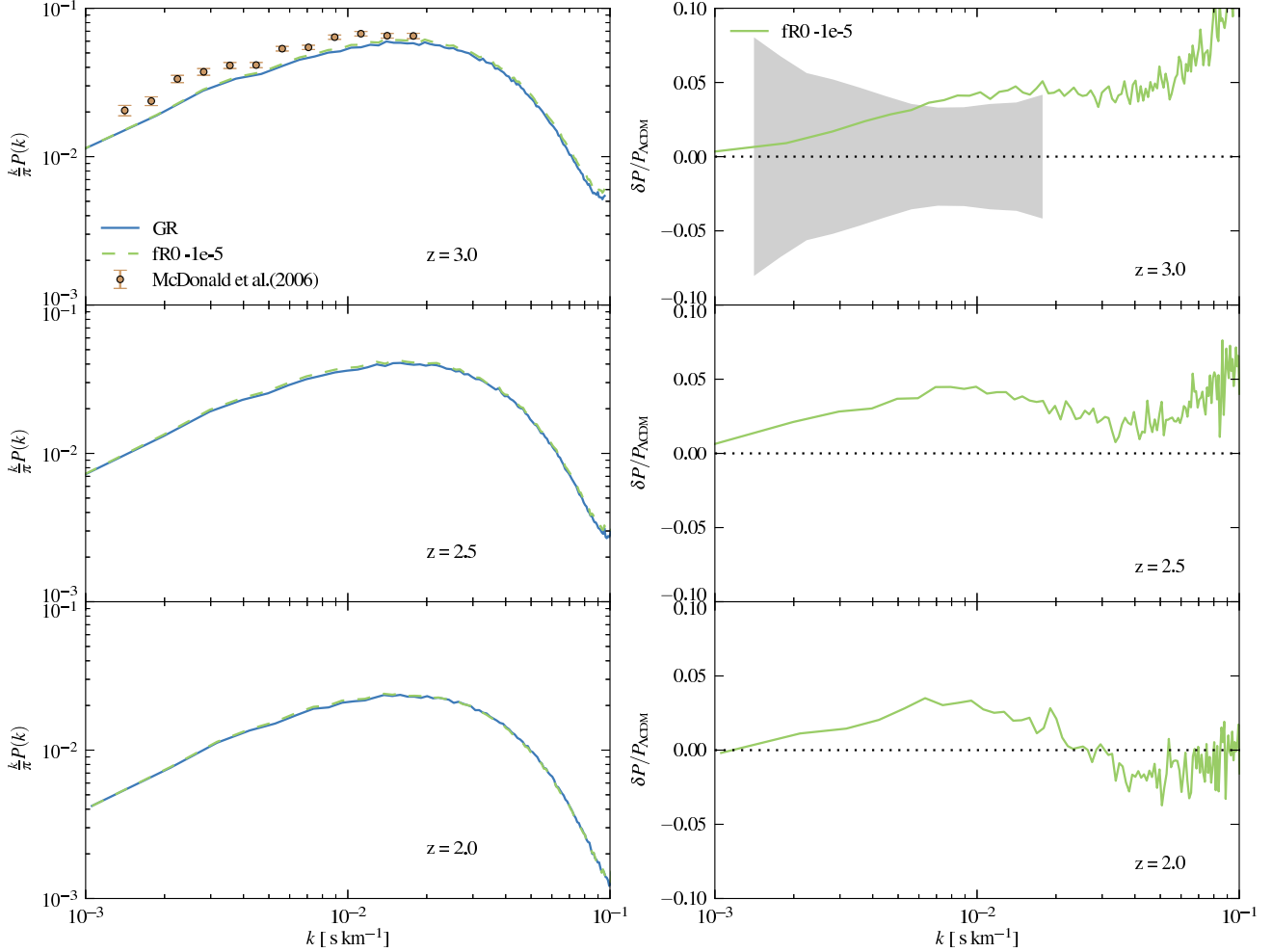


**Figure 2.** *Left panel:* Flux power spectra for  $f(R)$ -gravity and  $\Lambda$ CDM obtained from the  $60 h^{-1}\text{Mpc}$  simulation boxes at different redshifts. The dots with errorbars show the results of McDonald et al. (2006). *Right panel:* relative difference in the flux power spectra shown on the left hand side. The shaded area represents the relative errors of the McDonald et al. (2006) results at  $z = 3$ . The mean transmission is tuned to the values of Kim et al. (2007) for both panels.

they add a scalar function  $f(R)$  to the action:

$$S = \int d^4x \sqrt{-g} \left[ \frac{R + f(R)}{16\pi G} + \mathcal{L}_m \right], \quad (1)$$

where  $\mathcal{L}_m$  is the matter density Lagrangian,  $G$  is the gravitational constant and  $g$  is the determinant of the metric. As in GR, the field equations are obtained by variation with respect to the metric, leading to the so called *modified Einstein's equations* (Buchdahl 1970):

$$G_{\mu\nu} + f_R R_{\mu\nu} - \left( \frac{f}{2} - \square f_R \right) g_{\mu\nu} - \nabla_\mu \nabla_\nu f_R = 8\pi G T_{\mu\nu}. \quad (2)$$

$f_R = \frac{df(R)}{dR}$  denotes the derivative of the scalar function  $f(R)$  with respect to the Ricci scalar.

In order to simplify the above equation one can use the quasi-static approximation and neglect time derivatives if only scales much smaller than the horizon are considered (Oyaizu 2008; Noller et al. 2014). In addition, the calculations can be restricted to models with  $|f_R| \ll 1$ , as only

these are compatible with observations, giving (Oyaizu 2008, also see the Appendix of Arnold et al. 2014 for a detailed derivation):

$$\nabla^2 f_R = \frac{1}{3}(\delta R - 8\pi G \delta \rho). \quad (3)$$

$\delta R$  and  $\delta \rho$  denote the perturbations to the Ricci-scalar and the matter density with respect to the mean background values at a given time  $a$ .

To complete the set of differential equations for  $f(R)$ -gravity in the Newtonian limit, a modified Poisson equation for the gravitational potential can be derived from equation (2) (Hu & Sawicki 2007, see Arnold et al. 2014 for a more detailed derivation):

$$\nabla^2 \Phi = \frac{16\pi G}{3} \delta \rho - \frac{1}{6} \delta R. \quad (4)$$

To simulate the evolution of matter in the Universe in  $f(R)$ -gravity, equations (3) and (4) have to be solved. But first, the function  $f(R)$  needs to be specified. It should be chosen such that it meets the following requirements: First of all,

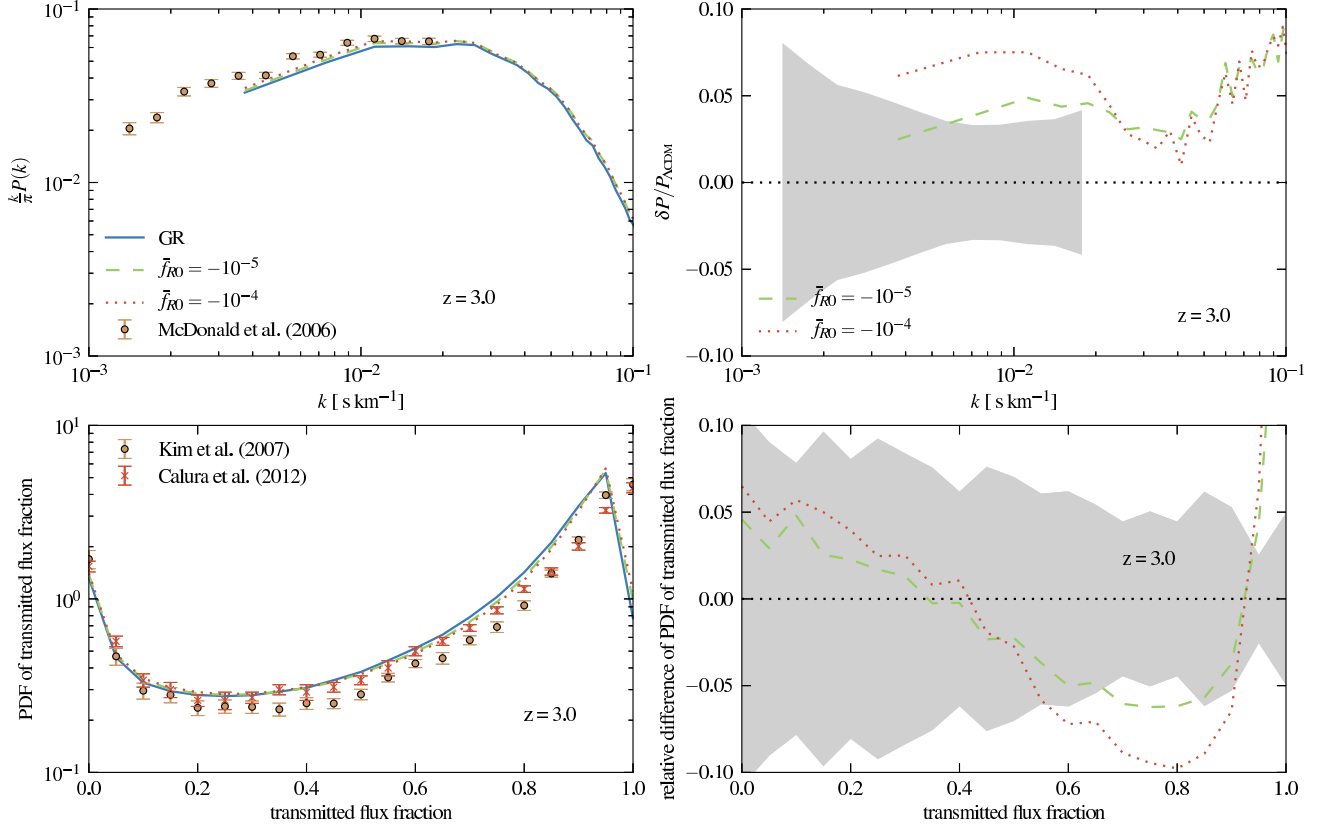


**Figure 3.** *Top panels:* Same as Figure 2. *Bottom panels:* same as Figure 1. In contrast to the previous figures the results are obtained from the  $15 h^{-1}$  Mpc simulation boxes and for both  $|\bar{f}_{R0}| = 10^{-4}$  and  $10^{-5}$ .

the model should reproduce the well constrained expansion history of a  $\Lambda$ CDM universe. And second, the  $f(R)$  modifications of ordinary gravity should be screened in high density regions, because GR appears valid to high accuracy in our local environment.

A model which is exactly designed to meet these requirements was proposed by Hu & Sawicki (2007):

$$f(R) = -m^2 \frac{c_1 \left(\frac{R}{m^2}\right)^n}{c_2 \left(\frac{R}{m^2}\right)^n + 1}, \quad (5)$$

where  $m^2 \equiv H_0^2 \Omega_m$ . It produces a chameleon mechanism which ensures that high curvature regions like our local environment are screened from  $f(R)$  effects and thus experience the same forces as in GR.

The model reproduces the expansion history of  $\Lambda$ CDM if one chooses the parameters  $c_1$  and  $c_2$  according to (Hu & Sawicki 2007):

$$\frac{c_1}{c_2} = 6 \frac{\Omega_\Lambda}{\Omega_m} \quad \text{and} \quad c_2 \left(\frac{R}{m^2}\right)^n \gg 1. \quad (6)$$

$n$  will be set to 1 for all simulations in this work. The remaining free parameter can be expressed in a more convenient way as follows. For a given choice of parameters, the derivative of  $f(R)$  with respect to  $R$  reads:

$$f_R = -n \frac{c_1 \left(\frac{R}{m^2}\right)^{n-1}}{\left[c_2 \left(\frac{R}{m^2}\right)^n + 1\right]^2} \approx -n \frac{c_1}{c_2^2} \left(\frac{m^2}{R}\right)^{n+1}, \quad (7)$$

again using  $c_2 \left(\frac{R}{m^2}\right)^n \gg 1$  for the second equality. Fixing the

metric to a Friedman-Lemaître-Robertson-Walker universe and assuming a flat  $\Lambda$ CDM expansion history, the background curvature is:

$$\bar{R} = 3m^2 \left[ a^{-3} + 4 \frac{\Omega_\Lambda}{\Omega_m} \right]. \quad (8)$$

With equation (8) one can now express the free parameter in terms of the background value of  $f_R$  at  $a = 1$ ,  $\bar{f}_{R0}$ . Together with equations (6) and (7),  $\Omega_m$ ,  $\Omega_\Lambda$ ,  $H_0$  and  $n$ ,  $\bar{f}_{R0}$  fully constrains the model and allows solving of the field equations.

### 3 SIMULATIONS AND METHODS

Modeling the statistical properties of the Lyman- $\alpha$  forest requires a cosmological simulation code which is capable of accounting for a variety of gas physics, including photoheating, radiative cooling and star formation. For  $f(R)$ -gravity, the fifth force influence has to be computed in addition. In this work, we use the modified gravity simulation code *Modified-Gravity-GADGET* (MG-GADGET, Puchwein et al. 2013), which is an extension of P-GADGET3, which in turn is an advanced version of GADGET2 (Springel 2005). Featuring the gas-physics modules of P-GADGET3 as well as a modified gravity solver, MG-GADGET offers the possibility to analyze the Lyman- $\alpha$  forest in the Hu & Sawicki (2007) model of  $f(R)$ -gravity, including nonlinear effects caused by the chameleon mechanism.

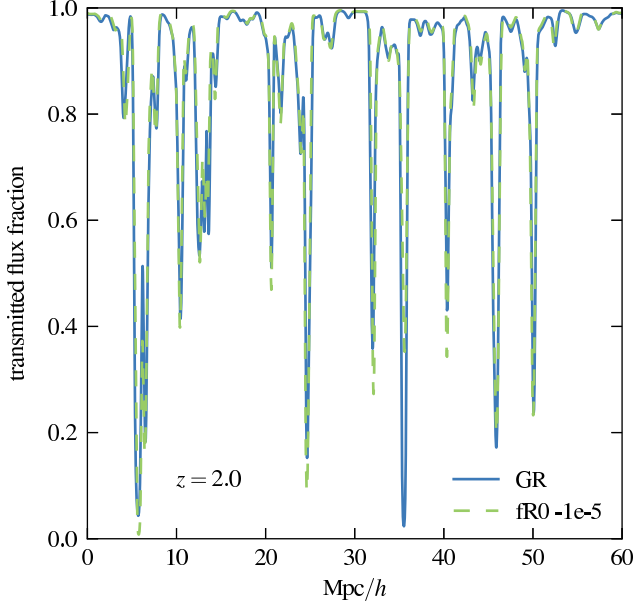


**Figure 4.** Transmitted flux fraction along an arbitrarily selected line of sight at  $z = 2$  for GR and  $|\bar{f}_{R0}| = 10^{-5}$ .

MG-GADGET solves the  $f(R)$ -equations as follows (for full details of the code functionality, see Puchwein et al. 2013): First, equation (3) is solved using an iterative Newton-Gauss-Seidel relaxation scheme. The iterations are carried out on an adaptively refining mesh so that an increased resolution is available in high density regions without causing a great loss of performance. Solving for  $f_R$  directly could lead to positive values for  $f(R)$  due to the finite iteration step-size. Because this would immediately stop the simulations, the code solves for  $u \equiv \ln(f_R/\bar{f}_R(a))$  instead (following Oyaizu 2008), and then calculates  $f$  from  $u$ . This iterative scheme is well suited for the highly nonlinear behavior of  $f_R$ .

As soon as the value for  $f_R$  is known, one can rewrite the modified Poisson equation in the form

$$\nabla^2 \Phi = 4\pi G(\delta\rho + \delta\rho_{\text{eff}}), \quad (9)$$

where

$$\delta\rho_{\text{eff}} = \frac{1}{3}\delta\rho - \frac{1}{24\pi G}\delta R, \quad (10)$$

is an effective density perturbation. Calculating  $\delta R$  through equation (7), the effective mass density is obtained. Adding the effective density to the real mass density, the standard TreePM gravity solver of P-GADGET3 can be used to solve equation (9) and calculate the gravitational forces on the individual particles, including  $f(R)$  effects. Note that all nonlinearities of the model are already encoded in  $\delta\rho_{\text{eff}}$  during this step. The hydrodynamical forces are calculated using the smoothed particle hydrodynamics (SPH) method implemented in P-GADGET3 (Springel & Hernquist 2002).

For a reliable analysis of  $f(R)$ 's impact on the Lyman- $\alpha$  forest it is necessary to run simulations in both modified gravity and  $\Lambda$ CDM using identical initial conditions. We do so by carrying out hydrodynamical simulations using  $2 \times 512^3$  particles ( $512^3$  each gas and dark matter) in a  $60 h^{-1}\text{Mpc}$  box for  $|\bar{f}_{R0}| = 10^{-5}$  and GR. To explore the parameter space at a coarse level, we also did

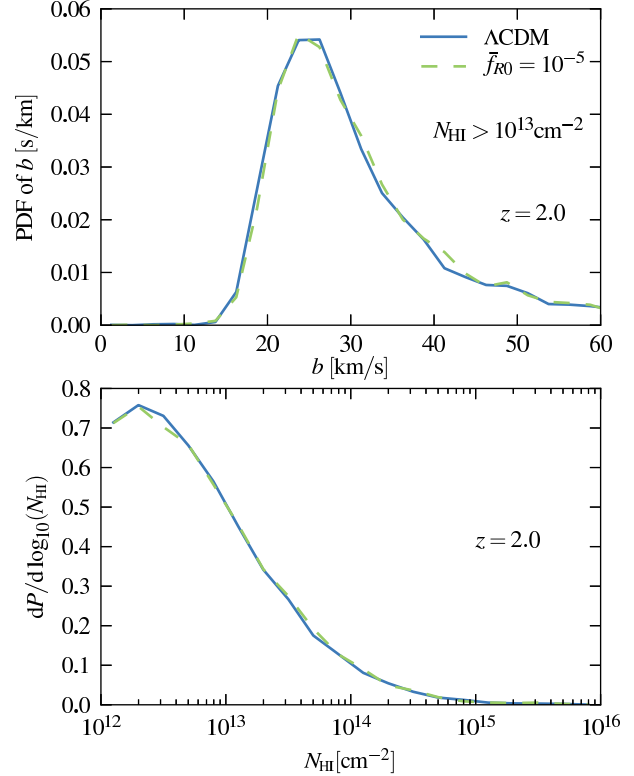


**Figure 5.** *Upper panel:* PDF of the linewidths of the Voigt profile fits to the Lyman- $\alpha$  absorption lines in the synthetic spectra for all lines with neutral hydrogen column density  $N_{\text{HI}} > 10^{13}\text{cm}^{-2}$  at  $z = 2$ . *Lower panel:* normalized PDF of the column density, considering all lines with  $N_{\text{HI}} > 10^{12}\text{cm}^{-2}$  at the same redshift. The spectra for both panels were tuned to the mean transmission of Becker et al. (2013) and were calculated from the  $60 h^{-1}\text{Mpc}$  simulations.

a set of smaller box simulations at the same mass resolution, but using  $2 \times 128^3$  particles in a  $15 h^{-1}\text{Mpc}$  box for  $|\bar{f}_{R0}| = 10^{-4}, 10^{-5}$  and GR. Our set of cosmological parameters is  $\Omega_m = 0.305, \Omega_\Lambda = 0.695, \Omega_b = 0.048$  and  $H_0 = 0.679$ , consistent with CMB constraints.

To extract the statistical properties of the Lyman- $\alpha$  forest, synthetic absorption spectra were calculated at different redshifts. Using the output of the hydrodynamical simulations, we randomly select 5000 lines-of-sight (LOS), each intersecting the simulation box parallel to one of the three coordinate axes. Dividing each line into 2048 pixels, the density of the neutral hydrogen, the gas temperature and the neutral gas weighted velocity fields of the gas are computed along the lines of sight. For this computation, we consider all SPH particles whose smoothing length is intersected by the sight-line. With the bulk flow velocities and temperatures along the line of sight in hand, we then account for kinematic Doppler shifts and thermal broadening of the absorption lines, which are themselves calculated from the neutral hydrogen density. As final output, the code creates for each LOS a file with optical depth  $\tau$  as a function of distance along the LOS. This output can be converted into a transmitted flux  $F = e^{-\tau}$ .

In the simulations, MG-GADGET uses a tabulated UV-

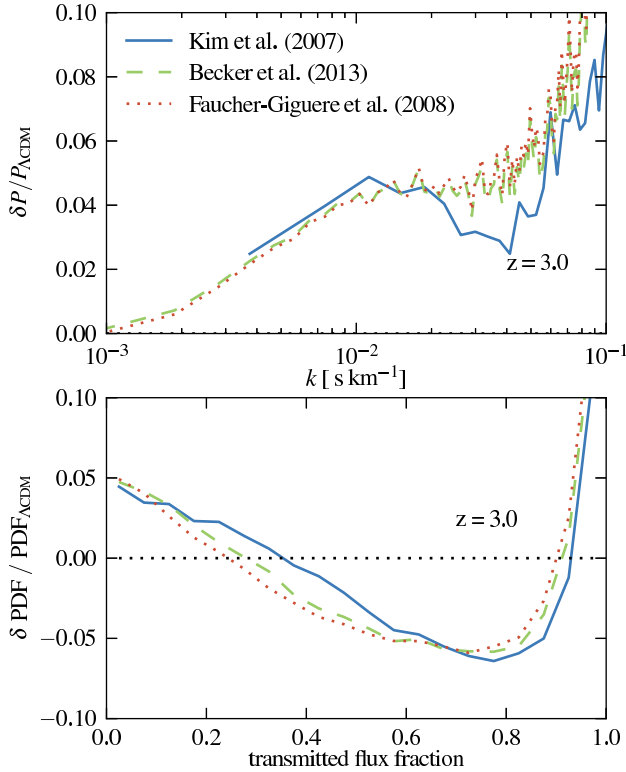


**Figure 6.** *Upper panel:* relative difference between  $f(R)$  and  $\Lambda$ CDM in the Lyman- $\alpha$  flux power spectrum; *lower panel:* relative difference between modified gravity and GR in the PDF of the transmitted flux fraction. For both plots, the values of the mean transmitted flux were tuned either to Kim et al. (2007, *blue solid line*), Becker et al. (2013, *green dashed line*), or Faucher-Giguere et al. (2008, *brown dotted line*), respectively. The results refer to  $z = 3$ .

background<sup>1</sup> which allows the calculation of gas temperatures and ionization fractions assuming ionization equilibrium. The results might however not fit the mean Lyman- $\alpha$  flux transmission actually seen in the observational data. In order to compare the mock spectra to observations more faithfully, it is therefore necessary to tune the mean transmitted flux to the corresponding value obtained in the observations. We perform this rescaling of the optical depths, which is a standard procedure in theoretical studies of the Lyman- $\alpha$  forest, in our post-processing of the LOS data.

#### 4 RESULTS

In analyzing the synthetic Lyman- $\alpha$  absorption spectra, we first consider the PDF of the transmitted flux fraction in the  $60 h^{-1} \text{Mpc}$  box simulations for both  $|\bar{f}_{R0}| = 10^{-5}$  and  $\Lambda$ CDM. Figure 1 shows these PDFs at redshifts  $z = 2, 2.5$  and  $3$  (*left hand panels*), as well as the relative differences between the two cosmological models (*right hand panels*).

<sup>1</sup> Taken from Haardt & Madau (2012), however with the He II photoheating rate boosted by a factor 1.7 for  $2.2 < z < 3.4$ . This slight modification results in a better agreement with observational constraints (Becker et al. 2011) on the temperature of the intergalactic medium.

The mean transmitted flux fraction is tuned in this plot to the observational values of Kim et al. (2007). We also show this data in the panels on the left hand side and its relative errors on the right hand side, for reference. In addition, the results of Calura et al. (2012) are shown for redshift  $z = 3$ . In both observations metal lines were excised, in the latter also Lyman-limit systems (LLS). The mean transmission measured by Calura et al. (2012) is consistent with the one of Kim et al. (2007). We can thus compare to the same theoretical prediction.

Comparing the absolute values, it is obvious that, despite the tuning to the same effective  $\bar{\tau}$ , the simulation results do not match the observations particularly well. Especially at redshift  $z = 3$ , the gap between the simulation results of both  $f(R)$  gravity and GR and the observational values of Kim et al. (2007) is much larger than the errorbars. At intermediate fluxes, the Calura et al. (2012) results are much closer to the simulations. Nevertheless, the differences at large transmitted flux fractions clearly exceed the  $3\sigma$  observational error. Considering the panels for redshift  $z = 2$  and  $2.5$ , the discrepancies between simulations and the observational data are smaller, but in certain regimes still larger than  $3\sigma$ . These differences might have their origin in the still uncertain systematic errors of observations (like, e.g., in the continuum placement) and simulations, in an underestimate of the statistical errors (Rollinde et al. 2013) or in an unaccounted heating of the very low-density intergalactic medium (Bolton et al. 2008; Viel et al. 2009) by radiative transfer (McQuinn et al. 2009; Compostella et al. 2013) and non-ionization-equilibrium (Puchwein et al. 2014) effects or, as recently suggested, by TeV blazars (Broderick et al. 2012; Puchwein et al. 2012).

The difference between  $|\bar{f}_{R0}| = 10^{-5}$  and  $\Lambda$ CDM is much smaller than the difference between the simulation results and the observed values and somewhat smaller than the errorbars of the observations. This is even more obvious in the right hand panels of Figure 1. Comparing the relative difference in the flux PDF between  $f(R)$  and GR, it turns out that the differences between the models are mostly within the observational errors for individual flux bins for all considered redshifts. The overall deviation over many flux bins and redshifts could, however, still be statistically significant if systematic effects were better understood. Given the current uncertainties in Lyman- $\alpha$  forest studies and the already very tight constraints on the Hu & Sawicki (2007) model of  $f(R)$  gravity from other observables, it will therefore be hard to get competitive constraints on  $|\bar{f}_{R0}|$  using the flux PDF of the Lyman- $\alpha$  forest.

We arrive at a similar conclusion for the Lyman- $\alpha$  flux power-spectra obtained for the large simulation box: Figure 2 shows their absolute value for both  $f(R)$  gravity and a  $\Lambda$ CDM cosmology as well as the relative difference between these models. The theoretical results from our synthetic spectra are again tuned to the mean transmission of Kim et al. (2007). For  $z = 3$ , the simulation values are compared to the observational results of McDonald et al. (2006), with the gray shaded area in the relative difference plot indicating their quoted errors.

As for the flux PDF, the discrepancy between simulations and observations at redshift  $z = 3$  is quite large, in particular much larger than the errors given in McDonald et al. (2006). This might have its origin in systematic uncertain-



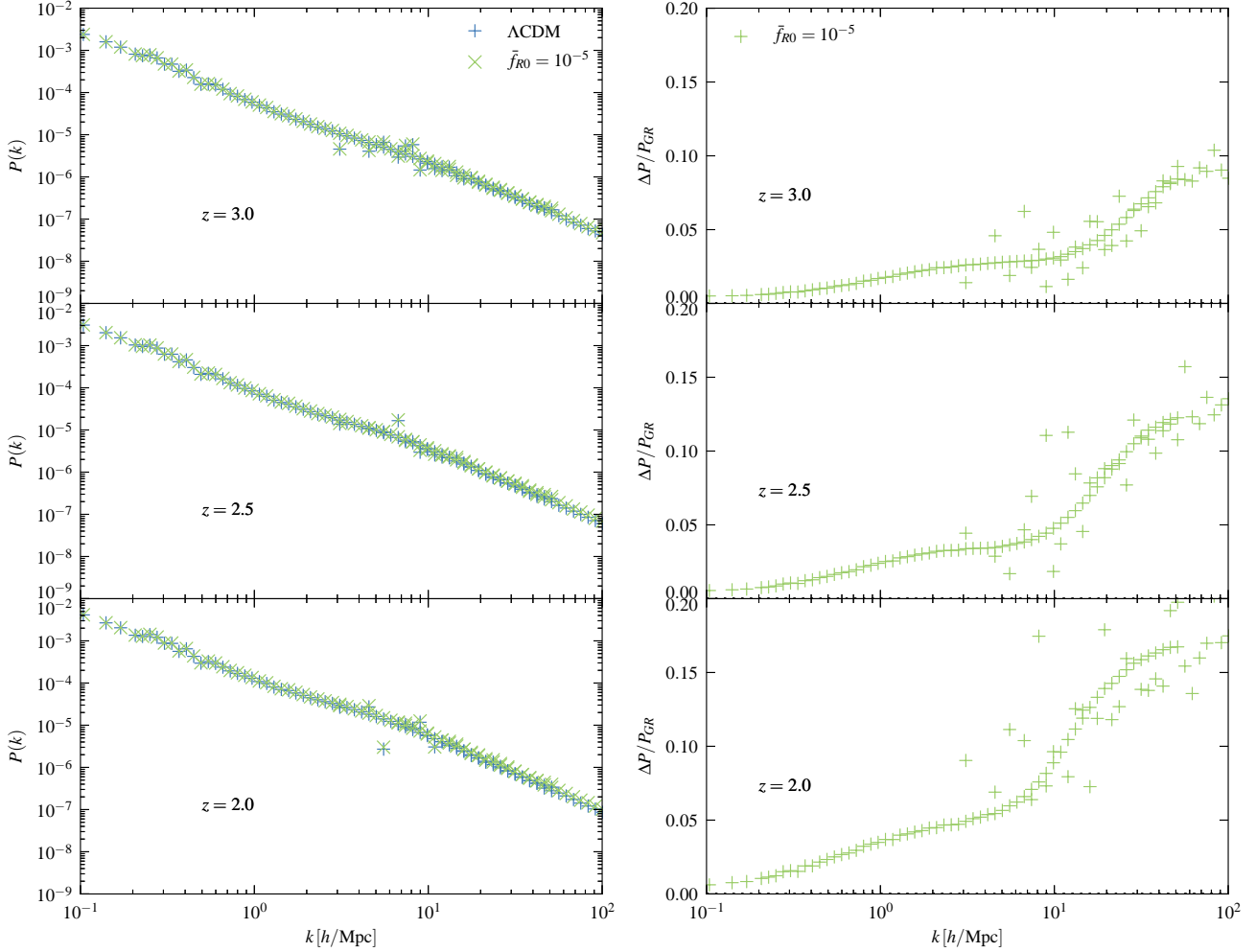


**Figure 7.** *Left Panel:* matter power spectrum for  $\Lambda\text{CDM}$  and  $|\bar{f}_{R0}| = 10^{-5}$  at three different redshifts. *Right panel:* Corresponding relative difference in the power spectra  $(P_{f(R)} - P_{GR})/P_{GR}$  between  $f(R)$  and GR.

ties which are not considered by the errorbars. Again, the difference between the two gravitational models is tiny, compared to the difference between observational data and the results from the simulations. Because the difference to GR is again smaller than or comparable to the errorbars of the shown observations, we need to conclude that the Lyman- $\alpha$  flux power-spectrum is only mildly affected by  $f(R)$ -gravity.

This is also particularly evident in the relative difference plots at the right hand side. The difference in the flux power-spectrum between  $|\bar{f}_{R0}| = 10^{-5}$  and GR is about 5% at maximum, considering redshifts  $z = 2, 2.5$  and 3. Normalizing the results of McDonald et al. (2006) to our  $\Lambda\text{CDM}$  outcome, it is obvious that the relative difference between the  $f(R)$  simulation results and the fiducial model is consistent with the relative errors quoted for the individual  $k$  bins. The overall deviation over many bins and redshifts may be statistically significant. However, systematic effects would need to be better understood to obtain interesting constraints on  $\bar{f}_{R0}$  based on such observations.

To test if it is at all possible to constrain  $f(R)$  gravity using the Lyman- $\alpha$  forest, we also run a set of simula-

tions with smaller box size at equal mass and spatial resolution, for  $|\bar{f}_{R0}| = 10^{-4}, 10^{-5}$  and GR. The power spectra and flux PDFs at redshift  $z = 3$  are shown in Figure 3. For both power spectra and the PDFs, the results for GR and  $|\bar{f}_{R0}| = 10^{-5}$ , as well as their relative differences, are compatible with the values from the bigger simulation box shown in Figures 1 and 2. One can therefore conclude that the smaller box runs are sufficient for an analysis over the shown range of values. In the  $|\bar{f}_{R0}| = 10^{-4}$  simulations, the flux power spectrum does not fit the observed values of McDonald et al. (2006) despite tuning the mean transmission. As the absolute value of the Lyman- $\alpha$  power spectrum is not known with great accuracy, one should not overestimate the, compared to the over gravitational models, smaller difference of the  $|\bar{f}_{R0}| = 10^{-4}$  curve to the observations. Again, normalizing the GR results to the observations, one can compare the observational errors to the differences between  $f(R)$  and a  $\Lambda\text{CDM}$  universe. At intermediate scales the difference between  $|\bar{f}_{R0}| = 10^{-4}$  and GR is larger than for  $|\bar{f}_{R0}| = 10^{-5}$ . Nevertheless it does not exceed the  $2\sigma$  relative error of the observations for individual  $k$  bins. Given

that  $|\bar{f}_{R0}| = 10^{-4}$  appears already clearly ruled out by other methods (Lombriser et al. 2012a,b; Smith 2009; Schmidt et al. 2009; Dossett et al. 2014), it does not seem that current Lyman- $\alpha$  data can add much new information here.

Figure 3 also shows the PDF of the transmitted flux for the three different gravity models. As for the power spectrum, the  $|\bar{f}_{R0}| = 10^{-4}$  values do not fit the data much better than the other models at  $z = 3$ . Comparing relative errors to the difference between the models, we see that the difference between  $|\bar{f}_{R0}| = 10^{-4}$  and GR lies within the  $1\sigma$ -error region for almost all values. Only between a transmitted flux fraction of 0.6 and 0.9 the difference is larger than  $1\sigma$  and reaches about  $2\sigma$  at maximum. The flux PDF does therefore also not seem to be very competitive with current observational data compared to other methods to constrain  $\bar{f}_{R0}$ .

In comparison to other uncertainties in the cosmological model, the impact of  $f(R)$  gravity on Lyman- $\alpha$  flux power spectra or PDFs is fairly small, even if one considers quite extreme and already excluded values for  $|\bar{f}_{R0}|$ .

Figure 4 illustrates how small the modified gravity effect on the Lyman- $\alpha$  forest is. It displays the transmitted flux fraction along an arbitrarily selected line of sight for  $f(R)$  and  $\Lambda$ CDM as a function of distance along this line. The positions of the absorption lines are the same for both models, as identical initial conditions have been used in both simulations. While there appear slight differences in the transmitted flux fractions for the individual absorption lines, no general pattern can be identified from a visual inspection.

Taking a more systematic approach, we used the code AutoVP (Davé et al. 1997) to fit Voigt-profiles to the absorption lines of the synthetic spectra. The PDF of the linewidth of the fitted Voigt-profiles is shown in the upper panel of Figure 5 for all lines with a neutral hydrogen column density  $N_{\text{HI}} > 10^{13} \text{ cm}^{-2}$  at redshift  $z = 2$ . As the lines almost perfectly overlap each other, it is perhaps not surprising that there is no significant difference in the linewidth distributions between  $f(R)$  gravity and a  $\Lambda$ CDM universe. The lower panel of the figure displays the normalized column density PDF of the absorption lines. As for the linewidth, the difference between the curves for  $|\bar{f}_{R0}| = 10^{-5}$  and the  $\Lambda$ CDM model is negligible.

The absolute values of the statistical Lyman- $\alpha$  measures depend on the observational value the mean transmitted flux is tuned to. To justify our previous analysis, we briefly show that the relative differences do not depend strongly on the actual value that is adopted. Figure 6 shows the relative difference in flux PDF and power spectrum between  $|\bar{f}_R| = 10^{-5}$  and GR. Each line in the plot is tuned to a different mean  $\tau$ , representing the observational data of Becker et al. (2013), Kim et al. (2007) and Faucher-Giguère et al. (2008). The figure shows that neither the relative difference in the power spectra nor the flux PDF do strongly depend on the choice of the tuning value for  $z = 3$ . As our analysis confirms, this does also hold for  $z = 2$  and 2.5. One can therefore conclude that the relative differences can be explored safely despite the fact that the absolute values depend on the actual value used for the mean transmission.

To complement our analysis of the Lyman- $\alpha$  forest in the simulations, we also analyzed the total matter power spectra at different redshifts. Figure 7 shows these spectra for  $|\bar{f}_R| = 10^{-5}$  and  $\Lambda$ CDM scenarios at redshifts  $z = 2, 2.5$

and 3, as well as the relative difference between the models. Comparing the power spectrum enhancement to previous works, our results at redshift  $z = 2$  are in good agreement with those of Li et al. (2013). The evolution of the enhancement with time in our simulations is consistent with previous works, too (Li et al. 2013; Winther & Ferreira 2014). This confirms that our  $f(R)$  simulations feature an impact of modified gravity at the expected level, even though the effects on the Lyman- $\alpha$  forest properties are weak.

Comparing matter and flux power spectra at the same scale, the relative differences between  $f(R)$  and GR are of similar size. The matter power spectra exhibit larger differences at smaller scales. There the Lyman- $\alpha$  flux power spectrum becomes, however, degenerate with uncertainties in the temperature of the intergalactic medium. Other gas properties like the temperature of gas in collapsed objects typically show  $f(R)$  effects of order 30% in the unscreened regime (Arnold et al. 2014). This also illustrates that the impact of  $f(R)$  gravity on the Lyman- $\alpha$  forest is rather small in comparison. In order to constrain  $f(R)$ , it therefore appears more promising to focus on other measures of structure growth rather than the Lyman- $\alpha$  forest.

## 5 SUMMARY AND CONCLUSIONS

In this work, we analyzed the statistical properties of the Lyman- $\alpha$  forest and the matter power spectra in hydrodynamical cosmological simulations of  $f(R)$  gravity. Our simulations employed the Hu & Sawicki (2007) model and used the modified gravity simulation code MG-GADGET. For comparison, we also ran a set of simulations for a  $\Lambda$ CDM universe. Our main findings can be summarized as follows:

- The PDF of the transmitted Lyman- $\alpha$  flux fraction is only mildly affected by  $f(R)$  gravity. The maximum relative difference between  $|\bar{f}_{R0}| = 10^{-5}$  and GR is of order 7%. For  $|\bar{f}_{R0}| = 10^{-4}$  the difference grows to at most 10%. The simulation results do not fit the observational data of Kim et al. (2007) at all redshifts, regardless of the gravitational model. If the observations are normalized to the GR results from the simulations, the relative differences between the gravitational models do not exceed the  $2\sigma$  relative error of the observations. For  $z = 3$ , the Calura et al. (2012) data matches the simulation results at intermediate transmitted flux fractions much better. This highlights that the present observational data is relatively uncertain. At high transmissions there are also significant deviations.
- For the flux power spectra we arrive at similar results. The relative difference between the models reaches at most 5% for  $|\bar{f}_{R0}| = 10^{-5}$  and about 10% for  $|\bar{f}_{R0}| = 10^{-4}$ . Again, the differences to GR for the stronger model are within the  $2\sigma$  relative error of the observational data (McDonald et al. 2006). Despite tuning the mean transmitted flux to the observational values, the power spectrum at  $z = 3$  does not accurately reproduce the observational data.
- There is no significant change in the shapes and abundances of absorption lines in  $f(R)$  modified gravity: Both the column density and line width distribution functions based on Voigt profile fitting do not exhibit any systematic change.
- The relative differences between  $f(R)$  and GR in the flux PDF and power spectra do not depend significantly on the observed mean transmission value to which the simulated



spectra are scaled. The tuning affects only the absolute values of these statistical Lyman- $\alpha$  measures.

- The matter power spectrum shows an enhancement in  $f(R)$  gravity which grows with time. The amplitude of the effect and the relative difference to GR is consistent with previous works. These relative changes in the matter power spectrum are of comparable magnitude as the changes in the Lyman- $\alpha$  forest flux power spectrum at the same scale. Note, however, that the enhancement of the matter power spectrum continues to grow towards low redshift where it is no longer probed by the Lyman- $\alpha$  forest. Also, note that a much stronger influence of  $f(R)$  has been found for other gas properties like the gas temperature in collapsed objects in the unscreened regime as has been reported in Arnold et al. (2014).

All in all we arrive at the conclusion that the impact of  $f(R)$  gravity on the Lyman- $\alpha$  forest is small. The relative differences in flux PDFs and flux power spectra are only of the order of 5%. Even for likely excluded models, like  $|\bar{f}_{R0}| = 10^{-4}$ , the changes in the statistical Lyman- $\alpha$  forest properties do not exceed the relative errors of available observations in individual flux or wavenumber bins. Using the full data over a range of redshifts a detection of modified gravity effects could probably be statistically significant due to its clearly defined signature. However, currently, systematic effects do not seem to be understood at the required level to get competitive constraints in practice. One can therefore conclude that Lyman- $\alpha$  forest properties are of limited discriminative power to constrain  $|\bar{f}_{R0}|$  at the moment. The remarkable robustness of the forest statistics has however also advantages. Given that the considered gravitational models have a negligible impact on the Lyman- $\alpha$  forest compared to other cosmological and astrophysical uncertainties, it may not be necessary to consider  $|\bar{f}_{R0}|$  as an additional parameter in constraining cosmological parameters based on the Lyman- $\alpha$  forest.

## 6 ACKNOWLEDGEMENTS

C.A. and V.S. acknowledge support from the Deutsche Forschungsgemeinschaft (DFG) through Transregio 33, “The Dark Universe”. E.P. would like to thank Martin Haehnelt for helpful discussions and acknowledges support by the FP7 ERC Advanced Grant Emergence-320596.

## References

- Arnold C., Puchwein E., Springel V., 2014, MNRAS, 440, 833
- Becker G. D., Bolton J. S., Haehnelt M. G., Sargent W. L. W., 2011, MNRAS, 410, 1096
- Becker G. D., Hewett P. C., Worseck G., Prochaska J. X., 2013, MNRAS, 430, 2067
- Bolton J. S., Viel M., Kim T.-S., Haehnelt M. G., Carswell R. F., 2008, MNRAS, 386, 1131
- Broderick A. E., Chang P., Pfrommer C., 2012, ApJ, 752, 22
- Buchdahl H. A., 1970, MNRAS, 150, 1
- Cai Y.-C., Li B., Cole S., Frenk C. S., Neyrinck M., 2014, MNRAS, 439, 2978
- Calura F., Tescari E., D’Odorico V., Viel M., Cristiani S., Kim T.-S., Bolton J. S., 2012, MNRAS, 422, 3019
- Compostella M., Cantalupo S., Porciani C., 2013, MNRAS, 435, 3169
- Corbett Moran C., Teyssier R., Li B., 2014, arXiv: 1408.2856
- Davé R., Hernquist L., Weinberg D. H., Katz N., 1997, ApJ, 477, 21
- Dossett J., Hu B., Parkinson D., 2014, JCAP, 3, 46
- Faucher-Giguère C.-A., Prochaska J. X., Lidz A., Hernquist L., Zaldarriaga M., 2008, ApJ, 681, 831
- Ferraro S., Schmidt F., Hu W., 2011, Phys. Rev. D, 83, 063503
- Fontanot F., Puchwein E., Springel V., Bianchi D., 2013, MNRAS, 436, 2672
- Gasperini M., Piazza F., Veneziano G., 2002, Phys. Rev. D, 65, 023508
- Haardt F., Madau P., 2012, ApJ, 746, 125
- Hinterbichler K., Khoury J., 2010, Physical Review Letters, 104, 231301
- Hu W., Sawicki I., 2007, Phys. Rev. D, 76, 064004
- Jennings E., Baugh C. M., Li B., Zhao G.-B., Koyama K., 2012, MNRAS, 425, 2128
- Khoury J., Weltman A., 2004, Phys. Rev. D, 69, 044026
- Kim T.-S., Bolton J. S., Viel M., Haehnelt M. G., Carswell R. F., 2007, MNRAS, 382, 1657
- Lam T. Y., Nishimichi T., Schmidt F., Takada M., 2012, Physical Review Letters, 109, 051301
- Li B., Hellwing W. A., Koyama K., Zhao G.-B., Jennings E., Baugh C. M., 2013, MNRAS, 428, 743
- Li B., Zhao G.-B., Teyssier R., Koyama K., 2012, JCAP, 1, 51
- Li Y., Hu W., 2011, Phys. Rev. D, 84, 084033
- Llinares C., Mota D. F., Winther H. A., 2014, A&A, 562, A78
- Lombriser L., Koyama K., Zhao G.-B., Li B., 2012a, Phys. Rev. D, 85, 124054
- Lombriser L., Schmidt F., Baldauf T., Mandelbaum R., Seljak U., Smith R. E., 2012b, Phys. Rev. D, 85, 102001
- McDonald P. et al., 2006, ApJS, 163, 80
- McQuinn M., Lidz A., Zaldarriaga M., Hernquist L., Hopkins P. F., Dutta S., Faucher-Giguère C.-A., 2009, ApJ, 694, 842
- Noller J., von Braun-Bates F., Ferreira P. G., 2014, Phys. Rev. D, 89, 023521
- Oyaizu H., 2008, Phys. Rev. D, 78, 123523
- Puchwein E., Baldi M., Springel V., 2013, MNRAS, 436, 348
- Puchwein E., Bolton J. S., Haehnelt M. G., Madau P., Becker G. D., 2014, ArXiv e-print: 1410.1531
- Puchwein E., Pfrommer C., Springel V., Broderick A. E., Chang P., 2012, MNRAS, 423, 149
- Rollinde E., Theuns T., Schaye J., Pâris I., Petitjean P., 2013, MNRAS, 428, 540
- Schmidt F., 2010, Phys. Rev. D, 81, 103002
- Schmidt F., Lima M., Oyaizu H., Hu W., 2009, Phys. Rev. D, 79, 083518
- Smith T. L., 2009, arXiv: 0907.4829
- Springel V., 2005, MNRAS, 364, 1105
- Springel V., Hernquist L., 2002, MNRAS, 333, 649
- Vainshtein A., 1972, Physics Letters B, 39, 393
- Viel M., Bolton J. S., Haehnelt M. G., 2009, MNRAS, 399,

L39

Winther H. A., Ferreira P. G., 2014, arXiv:1403.6492

Zhao G.-B., Li B., Koyama K., 2011, Phys. Rev. D, 83,  
044007